

# Inclusive measurements of diffractive DIS at H1

Paul Thompson

School of Physics, University of Birmingham, Birmingham B15 2TT, UK

Received: 1 Dec 2003 / Accepted: 12 Dec 2003 /

Published Online: 17 Dec 2003 – © Springer-Verlag / Società Italiana di Fisica 2003

**Abstract.** Recent measurements of the diffractive cross section in deep-inelastic scattering (DIS) at HERA are presented. The data are used to investigate the factorisation properties of diffractive DIS and to examine its quantum chromodynamic (QCD) structure.

## 1 Diffractive deep inelastic scattering

At low  $x$  in DIS at HERA, approximately 10% of the events are of the type  $ep \rightarrow eXp$ , where the final state proton carries in excess of 95% of the proton beam energy [1]. The kinematics of these processes are illustrated in Fig. 1. A photon of virtuality  $Q^2$ , coupled to the electron, undergoes a strong interaction with the proton to form a final state hadronic system  $X$  (mass  $M_X$ ) separated by a large rapidity gap from the leading proton. No net quantum numbers are exchanged. A fraction  $x_P$  of the proton longitudinal momentum is transferred to the system  $X$ . The virtual photon couples to a quark carrying a fraction  $\beta$  of the exchanged momentum. The squared four-momentum transfer at the proton vertex is denoted  $t$ .

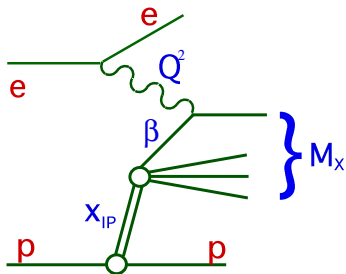


**Fig. 1.** Illustration of the kinematic variables used to describe diffractive DIS

Events with this ‘diffractive’ topology are interpreted in Regge models in terms of pomeron trajectory exchange between the proton and the virtual photon. The large photon virtualities encourage a perturbative QCD treatment of the process. However, the parton level interpretation is not obvious. In order to generate an exchange with net vacuum quantum numbers, a minimum of two partons must be exchanged in the  $t$  channel.

The differential cross section for diffractive DIS is often presented in terms of a diffractive structure function  $F_2^{D(4)}(\beta, Q^2, x_P, t)$ , defined analogously to the in-

clusive proton structure function  $F_2$ . The measurements presented here have been obtained by requiring an absence of particles in the forward region, where  $t$  is not directly measured. Therefore, the results are presented in the form of a structure function  $F_2^{D(3)}(\beta, Q^2, x_P)$ , corresponding to an integral of  $F_2^{D(4)}$  over  $t$ . The reduced cross section  $\sigma_r^{D(3)}(\beta, Q^2, x_P)$  is related to the diffractive structure functions  $F_2^{D(3)}(\beta, Q^2, x_P)$  and  $F_L^{D(3)}(\beta, Q^2, x_P)$  by

$$\sigma_r^{D(3)} = F_2^{D(3)} - \frac{y^2}{1 + (1 - y)^2} F_L^{D(3)}, \quad (1)$$

such that  $\sigma_r^{D(3)} \sim F_2^D$  except at very large values of  $y$ .

## 2 Factorisation properties and diffractive parton densities

The preliminary results presented here are based on data collected with the H1 detector in  $e^+p$  interactions at HERA at low [2], intermediate [3] and high [4] values of  $Q^2$ . In this section, these data are used to test the factorisation properties of diffractive DIS.

A NLO QCD fit [5] has been performed on the intermediate  $Q^2$  data. This fit was based on the hard scattering QCD factorisation theorem for diffraction [6], which implies that diffractive parton densities can be defined for diffractive DIS, such that at fixed  $x_P$  and  $t$ , the  $Q^2$  and  $\beta$  evolution is described by the DGLAP equations. The dependence on  $(\beta, Q^2)$  then represents a structure function for the exchanged pomeron [7]. In Fig. 2, the data are compared with the results of the fit for one example value of  $Q^2 = 6.5 \text{ GeV}^2$ . The fit is found to give a good description of the data across the large kinematic range covered by the measurements, and results in diffractive parton densities dominated by the gluon density, which extends to large fractional momenta.

The hard scattering factorisation proof [6] makes no prediction for the  $(x_P, t)$  dependence. From the QCD perspective, the diffractive parton densities could vary in both

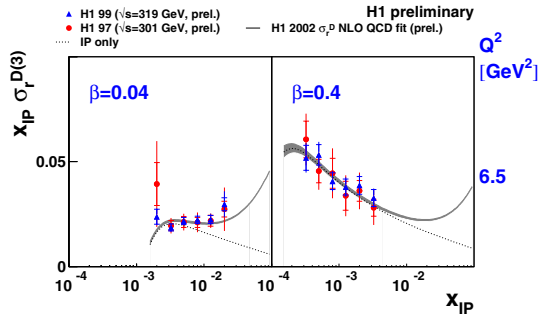


**Fig. 2.** Dependence of  $x_{\text{IP}} \sigma_r^{D(3)}$  on  $x_{\text{IP}}$  at fixed  $Q^2 = 6.5 \text{ GeV}^2$ , for two values of  $\beta$ . The data are compared with the NLO QCD fit

shape and normalisation with these variables. However, the success of Regge phenomenology in describing soft hadronic cross sections with a universal pomeron trajectory suggests that there may be an extended ‘Regge’ factorisation property, whereby the  $x_{\text{P}}$  dependence is driven by Regge asymptotics and is completely decoupled from the  $(\beta, Q^2)$  dependence. The Regge factorisation hypothesis is tested by measuring the data at a large number of  $x_{\text{P}}$  values and performing a fit with a parameterisation of the form

$$\sigma_r^{D(3)} = f_{\text{IP}}(x_{\text{P}}) A_{\text{IP}}(\beta, Q^2) + f_{\text{IR}}(x_{\text{P}}) A_{\text{IR}}(\beta, Q^2) \quad (2)$$

where  $f_{\text{IP}}(x_{\text{P}})$  and  $f_{\text{IR}}(x_{\text{P}})$  correspond to pomeron and sub-leading reggeon flux factors. The free parameters in the fit are the effective pomeron intercept  $\alpha_{\text{IP}}(0)$  and the coefficients  $A_{\text{IP}}(\beta, Q^2)$  and  $B_{\text{IR}}(\beta, Q^2)$  at each  $(\beta, Q^2)$  point. The fit yields  $\alpha_{\text{IP}}(0) = 1.173 \pm 0.018 \text{ (stat.)} \pm 0.017 \text{ (syst.)} {}^{+0.063}_{-0.035} \text{ (model)}$ , the dominant model dependence uncertainty arising from the unknown contribution of the cross section for longitudinally polarised photons. The Regge factorisation hypothesis works well within the kinematic range measured in [3], with no significant variation of the effective  $\alpha_{\text{IP}}(0)$  with  $\beta$  or  $Q^2$ . There is thus no experimental evidence at the present level of precision for a variation of the diffractive parton densities with  $x_{\text{P}}$ .

### 3 Dependence on $Q^2$ and $\beta$

In order to study the  $\beta$  and  $Q^2$  dependence of the data with high precision, the reduced cross section  $\sigma_r^{D(3)}$  is extracted at several values of  $x_{\text{P}}$ . The data are presented in Fig. 3 and 4 in the form  $\sigma_r^{D(3)}/f_{\text{IP}}(\text{IP})$ , where  $f_{\text{IP}}$  corresponds to the ‘pomeron flux’ used in the Regge and QCD fits (2). The data are compared with the results of the NLO DGLAP QCD fit. The similarity of the normalised reduced cross section, in the regions in which they overlap, indicates that the factorising of the  $x_{\text{P}}$  dependence is, indeed, a good approximation.

A striking feature of the data is the scaling violations with positive  $\partial \sigma_r^{D(3)} / \partial \ln Q^2$  throughout most of the phase space, becoming negative only at the highest measured values of  $\beta$ . This behaviour is in contrast to that observed

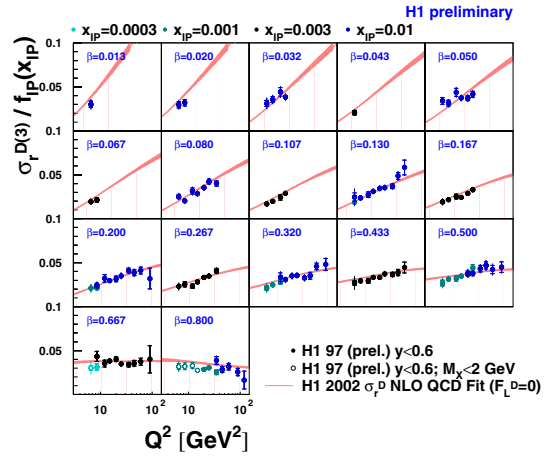


**Fig. 3.**  $Q^2$  dependence of the reduced cross section scaled by the values assumed for the  $t$ -integrated pomeron flux in the QCD fits. The data are compared with the prediction of the NLO QCD fit

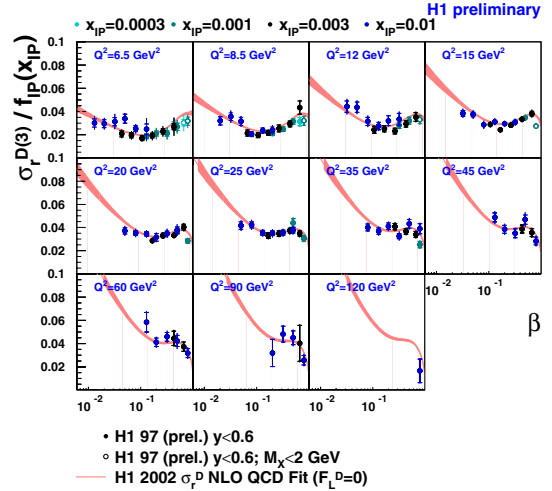


**Fig. 4.**  $\beta$  dependence of the reduced cross section scaled by the values assumed for the  $t$ -integrated pomeron flux in the QCD fits. The data are compared with the prediction of the NLO QCD fit

for the scaling violations of  $F_2(x, Q^2)$  at fixed  $x$ , which are negative for  $x \geq 0.1$ . In a QCD partonic interpretation, the scaling violations are suggestive of a large gluonic component of the diffractive exchange.

The  $\beta$  dependence of the reduced cross section at fixed  $x_{\text{P}}$  is relatively flat and remains large up to the highest fractional momenta of  $\beta = 1$ , again suggestive of a large gluonic component to the exchange. At the lowest  $Q^2$ , a rising behaviour of  $\sigma_r^{D(3)}$  with  $\beta$  is observed in the data as  $\beta \rightarrow 1$ , which becomes less pronounced with increasing  $Q^2$ . In a leading order QCD picture, the reduced cross section can be viewed as a charge weighted sum over the diffractive quark densities. The  $\beta$  and  $Q^2$  dependences are consistent with DGLAP evolution from high to low  $\beta$  with increasing  $Q^2$  due to gluon radiation.

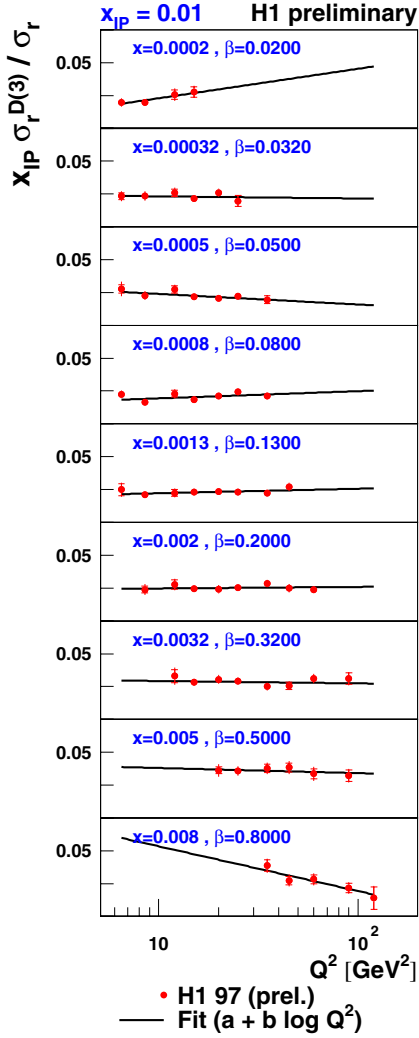


**Fig. 5.** The ratio of the diffractive cross section to the inclusive cross section as a function of  $Q^2$  for fixed  $x_P$  ( $x_P = 0.01$ ) for different values of  $x (= \beta \cdot x_P)$ . The curve shows a result of a fit of the form  $a + b \ln Q^2$

#### 4 The ratio of the diffractive to the inclusive cross section

The ratio of the diffractive to the inclusive cross section is extracted at fixed values of  $x_P$ , in order to compare the dynamics of diffractive DIS with those from inclusive DIS. The ratio, as a function of  $Q^2$  for one example  $x_P$  bin ( $x_P = 0.01$ ), is shown in Fig. 5. The ratio tests the difference between the scaling violations of  $\sigma_r^D$  and the inclusive cross section  $\sigma_r$ , when compared at the same  $x$ . At low values of  $\beta$  (or  $x$ ), the ratio is remarkably flat. At the highest  $\beta$ , where  $x$  approaches  $x_P$ , the ratio falls with increasing  $Q^2$ .

In order to quantify the  $Q^2$  dependence of the ratio, the logarithmic derivative  $b(x, x_P)$  is extracted from fits of the form

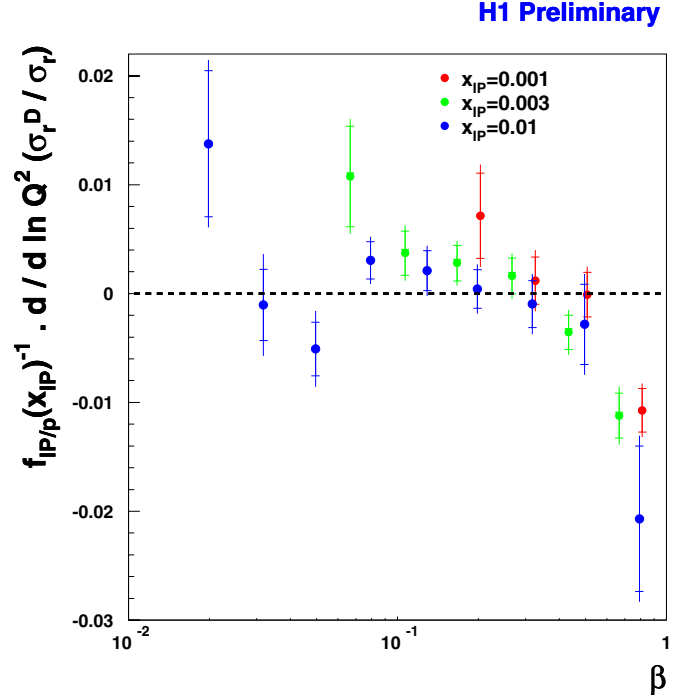


**Fig. 6.** Logarithmic  $Q^2$  derivatives of the ratio  $\sigma_r^D/\sigma_r$  for different  $\beta$  and  $x_P$  values, scaled at each  $x_P$  by the values assumed for the  $t$ -integrated pomeron flux in the QCD fits

$$\frac{\sigma_r^D(x_P, x, Q^2)}{\sigma_r(x, Q^2)} = a(x, x_P) + b(x, x_P) \ln Q^2 \quad (3)$$

The resulting values of the derivative are shown in Fig. 6 with the “pomeron flux” divided out, so that the results at different values of  $x_P$  can be compared. The  $Q^2$  dependences of the diffractive and inclusive cross sections are consistent with being the same away from  $x = x_P$  ( $\beta = 1$ ), suggesting that the two processes have similar underlying  $Q^2$  dynamics.

#### References

1. H1 Collaboration, C. Adloff et al.: *Z. Phys. C* **76**, 613 (1997)
2. H1 Collaboration: abstract 981, paper submitted to ICHEP2002, Amsterdam
3. H1 Collaboration: abstract 808, paper submitted to EPS Conference on HEP 2001, Budapest
4. H1 Collaboration: abstract 090, paper submitted to EPS Conference on HEP 2003, Aachen
5. H1 Collaboration: abstract 980, paper submitted to ICHEP2002, Amsterdam
6. J. Collins: *Phys. Rev. D* **57**, 3051 (1998), Erratum-ibid. **D 61**, 019902 (2000)
7. G. Ingelman and P. Schlein: *Phys. Lett. B* **152**, 256 (1985)